PROCEEDINGS OF SCIENCE

Current Status of ε_K in lattice QCD

Weonjong Lee[a,b,1,*]

[a] *Lattice Gauge Theory Research Center, CTP, and FPRD, Department of Physics and Astronomy, Seoul National University, Seoul 08826, South Korea*

[b] *School of Physics, Korea Institute for Advanced Study (KIAS), Seoul 02455, South Korea*

E-mail: wlee@snu.ac.kr

We present recent progress in ε_K (the indirect CP violation parameter in the neutral kaon system) determined directly from the standard model (SM) with lattice QCD inputs such as $\hat{B}_K$, $|V_{cb}|$, $|V_{us}|$, ξ_0, ξ_2, $\xi_{\rm LD}$, f_K, and m_c. We find that the standard model with exclusive $|V_{cb}|$ and other lattice QCD inputs describes only 65% of the experimental value of $|\varepsilon_K|$ and does not explain its remaining 35%, which leads to a strong tension in $|\varepsilon_K|$ at the 5.1σ level between the SM theory and experiment. We also find that this tension disappears when we use the inclusive value of $|V_{cb}|$ obtained using the heavy quark expansion based on the QCD sum rule approach, although this inclusive tension is small ($\approx 1.4\sigma$) but keeps increasing as time goes on.

Corfu Summer Institute 2022 "School and Workshops on Elementary Particle Physics and Gravity",
28 August - 1 October, 2022
Corfu, Greece

[1] The SWME collaboration
[*] Speaker

https://pos.sissa.it/

PoS(CORFU2022)028

1. Introduction

CP violation provides a natural window to search for new physics [1, 2]. In particular, the indirect CP violation in the neutral kaon system is highly sensitive to new physics, since the experimental results are very precise [3], and lattice QCD makes it possible to achieve a high precision on calculating physical observables in kaon physics. Here, we focus on the indirect CP violation.

Definition of the indirect CP violation parameter ε_K in neutral kaon system is

$$\varepsilon_K \equiv \frac{\mathcal{A}(K_L \to \pi\pi(I=0))}{\mathcal{A}(K_S \to \pi\pi(I=0))}\,, \tag{1}$$

where K_L and K_S are the neutral kaon states in nature, and $I = 0$ is the isospin of the final two-pion state. In experiment [3],

$$\begin{aligned}\varepsilon_K &= (2.228 \pm 0.011) \times 10^{-3} \times e^{i\phi_\varepsilon}\,,\\ \phi_\varepsilon &= 43.52 \pm 0.05^\circ\,.\end{aligned} \tag{2}$$

Here, we present recent progress in determining $|\varepsilon_K|$ with lattice QCD inputs, which is an update from our previous reports [4–11]. In order to calculate ε_K directly from the SM, we need to know 18 input parameters [7, 8]. Among them, input parameters coming from lattice QCD include $\hat{B}_K$, exclusive $|V_{cb}|$, $|V_{us}|$, ξ_0, ξ_2, $\xi_{\rm LD}$, f_K, and m_c.

Here, we follow the color convention of our previous papers [4, 5] in Tables. We use the red color for the new input data which is used to evaluate ε_K. We use the blue color for the new input data which is not used for some obvious reason.

2. Master Formula for ε_K

In the standard model (SM), the indirect CP violation parameter ε_K in the neutral kaon system can be re-expressed in terms of the well-known SM parameters as follows,

$$\begin{aligned}\varepsilon_K =& e^{i\theta}\sqrt{2}\sin\theta\Big(C_\varepsilon X_{\rm SD}\hat{B}_K + \frac{\xi_0}{\sqrt{2}} + \xi_{\rm LD}\Big)\\ &+ O(\omega\varepsilon') + O(\xi_0\Gamma_2/\Gamma_1)\,.\end{aligned} \tag{3}$$

This is the master formula, and its derivation is well explained in Ref. [8]. Here, we use the same notation and convention as in Ref. [7, 8].

2.1 Short Distance Contribution to ε_K

In the master formula of Eq. (3), the dominant leading-order effect ($\approx$ +107%) comes from the short distance (SD) contribution proportional to $\hat{B}_K$. Here, C_ε is a dimensionless parameter defined as:

$$C_\varepsilon \equiv \frac{G_F^2 F_K^2 m_{K^0} M_W^2}{6\sqrt{2}\pi^2 \Delta M_K} \cong 3.63 \times 10^4\,, \tag{4}$$

Here, $X_{\rm SD}$ represents the short distance effect from the Inami-Lim functions [12]:

$$X_{\rm SD} \equiv \operatorname{Im}\lambda_t \Big[\operatorname{Re}\lambda_c \eta_{cc} S_0(x_c) - \operatorname{Re}\lambda_t \eta_{tt} S_0(x_t) \\ - (\operatorname{Re}\lambda_c - \operatorname{Re}\lambda_t)\eta_{ct} S_0(x_c, x_t)\Big] \tag{5}$$

$$\cong 6.24 \times 10^{-8}\,, \tag{6}$$

where $\lambda_i = V_{is}^* V_{id}$ is a product of the CKM matrix elements with $i = u, c, t$, and η_{ij} with $i, j = c, t$ represent the QCD corrections of higher order in α_s [13]. There exists a potential issue with poor convergence of perturbation theory for η_{cc} at the charm scale, which is discussed properly in Ref. [8]. Here, S_0's are Inami-Lim functions [12] defined as

$$S_0(x_i) = x_i \left[\frac{1}{4} + \frac{9}{4(1-x_i)} - \frac{3}{2(1-x_i)^2} - \frac{3x_i^2 \ln x_i}{2(1-x_i)^3}\right],$$

$$S_0(x_i, x_j) = \left\{ \frac{x_i x_j}{x_i - x_j}\left[\frac{1}{4} + \frac{3}{2(1-x_i)} - \frac{3}{4(1-x_i)^2}\right] \ln x_i \right. \\ \left. + (i \leftrightarrow j)\right\} - \frac{3x_i x_j}{4(1-x_i)(1-x_j)}\,, \tag{7}$$

where $i = c, t$, $x_i = m_i^2/M_W^2$, and $m_i = m_i(m_i)$ is the scale invariant $\overline{\rm MS}$ quark mass. In $X_{\rm SD}$ of Eq. (5), the $S_0(x_t)$ term from the top-top contribution in the box diagrams describes about +72.4% of $X_{\rm SD}$, the $S_0(x_c, x_t)$ term from the top-charm contribution takes over about +45.4% of $X_{\rm SD}$, and the $S_0(x_c)$ term from the charm-charm contribution depicts about −17.8% of $X_{\rm SD}$.

Here, the kaon bag parameter $\hat{B}_K$ is defined as

$$\hat{B}_K \equiv B_K(\mu) b(\mu) \cong 0.76\,, \tag{8}$$

$$B_K(\mu) \equiv \frac{\langle \bar{K}^0 | O_{LL}^{\Delta S=2}(\mu) | K^0 \rangle}{\frac{8}{3}\langle \bar{K}^0 | \bar{s}\gamma_\mu\gamma_5 d | 0\rangle \langle 0 | \bar{s}\gamma^\mu\gamma_5 d | K^0\rangle} = \frac{\langle \bar{K}^0 | O_{LL}^{\Delta S=2}(\mu) | K^0 \rangle}{\frac{8}{3} F_K^2 m_{K^0}^2}\,, \tag{9}$$

$$O_{LL}^{\Delta S=2}(\mu) \equiv [\bar{s}\gamma_\mu(1-\gamma_5)d][\bar{s}\gamma^\mu(1-\gamma_5)d]\,, \tag{10}$$

where $b(\mu)$ is the renormalization group (RG) running factor to make $\hat{B}_K$ invariant with respect to the renormalization scale and scheme:

$$b(\mu) = [\alpha_s^{(3)}(\mu)]^{-2/9} K_+(\mu)\,. \tag{11}$$

Here, details on $K_+(\mu)$ are given in Ref. [8].

2.2 Long Distance Contribution to ε_K

There are two kinds of long distance (LD) contributions on ε_K: one is the absorptive LD effect from ξ_0 and the other is the dispersive LD effect from $\xi_{\rm LD}$. The absorptive LD effects are defined as

$$\tan \xi_0 \equiv \frac{\mathrm{Im}\, A_0}{\mathrm{Re}\, A_0} \,, \tag{12}$$

$$\tan \xi_2 \equiv \frac{\mathrm{Im}\, A_2}{\mathrm{Re}\, A_2} \,. \tag{13}$$

They are related with each other through ε':

$$\begin{aligned} \varepsilon' &\equiv e^{i(\delta_2-\delta_0)} \frac{i\omega}{\sqrt{2}} \Big(\tan \xi_2 - \tan \xi_0 \Big) \\ &= e^{i(\delta_2-\delta_0)} \frac{i\omega}{\sqrt{2}} (\xi_2 - \xi_0) + O(\xi_i^3) \,. \end{aligned} \tag{14}$$

The overall contribution of the ξ_0 term to ε_K is about -7%.

The dispersive LD effect is defined as

$$\xi_{\mathrm{LD}} = \frac{m'_{\mathrm{LD}}}{\sqrt{2}\Delta M_K} \,, \tag{15}$$

where

$$m'_{\mathrm{LD}} = -\mathrm{Im} \left[\mathcal{P} \sum_C \frac{\langle \overline{K}^0 | H_{\mathrm{w}} | C \rangle \langle C | H_{\mathrm{w}} | K^0 \rangle}{m_{K^0} - E_C} \right] \,. \tag{16}$$

if the CPT invariance is well respected. The overall contribution of the ξ_{LD} to ε_K is about ± 2%.

3. Input parameters

3.1 Input parameters: Wolfenstein parameters

The CKMfitter [14] and UTfit [15] collaborations provide the Wolfenstein parameters [16] (λ, $\bar{\rho}$, $\bar{\eta}$) obtained by the global unitarity triangle (UT) fit. The 2022 results are summarized in Table 1 (a). As explained in Refs. [7, 8], the Wolfenstein parameters extracted by the global UT fit have unwanted correlation with ε_K, since ε_K is used as an input to determine them. Hence, it is essential to avoid this unwanted correlation. One way to avoid it is that we may take another set of the Wolfenstein parameters determined from the angle-only-fit (AOF) suggested in Ref. [17]. In the AOF, they do not use ε_K, $\hat{B}_K$, and $|V_{cb}|$ as inputs to obtain the UT apex ($\bar{\rho}$, $\bar{\eta}$). Then, $|V_{us}|$ is used to determine λ, which comes from the $K_{\ell 2}$ and $K_{\ell 3}$ decays combined with lattice QCD results for form factors and decay constants as explained in Ref. [18]. The Wolfenstein parameter A is obtained directly from $|V_{cb}|$, which will be discussed later in Section 3.2.

In Table 1 (a), we present the most updated Wolfenstein parameters available in the market. As explained in Ref. [7, 11], we use the results of angle-only-fit (AOF) in Table 1 (a) to evaluate ε_K.

3.2 Input parameters: $|V_{cb}|$

In Table 2 (a) and (b), we present recently updated results for exclusive $|V_{cb}|$ and inclusive $|V_{cb}|$ respectively. In Table 2 (a), we summarize results for exclusive $|V_{cb}|$ obtained by various groups: HFLAV, BELLE, BABAR, FNAL/MILC, LHCb, and FLAG. Results from LHCb comes

WP	CKMfitter		UTfit		AOF	
λ	0.22475(25)	[14]	0.22500(100)	[15]	0.2249(5)	[18]
$\bar{\rho}$	0.1577(96)	[14]	0.148(13)	[15]	0.156(17)	[19]
$\bar{\eta}$	0.3493(95)	[14]	0.348(10)	[15]	0.334(12)	[19]

(a) Wolfenstein parameters

Input	Value	Ref.
η_{cc}	1.72(27)	[8]
η_{tt}	0.5765(65)	[20]
η_{ct}	0.496(47)	[21]

(b) η_{ij}

Table 1: (a) Wolfenstein parameters and (b) QCD corrections: η_{ij} with $i, j = c, t$.

channel	value	method	ref	source
ex-comb	39.25(56)	CLN	[24] p115e223	HFLAV-2021
$B \to D^* \ell \bar{\nu}$	39.0(2)(6)(6)	CLN	[25] erratum p4	BELLE-2021
$B \to D^* \ell \bar{\nu}$	38.9(3)(7)(6)	BGL	[25] erratum p4	BELLE 2021
$B \to D^* \ell \bar{\nu}$	38.40(84)	CLN	[26] p5t2	BABAR-2019
$B \to D^* \ell \bar{\nu}$	38.36(90)	BGL	[26] p5t1	BABAR-2019
$B \to D^* \ell \bar{\nu}$	38.40(78)	BGL	[22] p27e76	FNAL/MILC-2022
$B_s \to D_s^* \ell \bar{\nu}$	41.4(6)(9)(12)	CLN	[27] p15	LHCb-2020
$B_s \to D_s^* \ell \bar{\nu}$	42.3(8)(9)(12)	BGL	[27] p15	LHCb-2020
ex-comb	39.48(68)	comb	[18] p145	FLAG-2021

(a) Exclusive $|V_{cb}|$ in units of 10^{-3}.

channel	value	ref	source
kinetic scheme	42.16(51)	[28] p1	Gambino-2021
kinetic scheme	42.00(64)	[18, 29] p145	FLAG-2021
1S scheme	41.98(45)	[24] p110e208	HFLAV-2021

(b) Inclusive $|V_{cb}|$ in units of 10^{-3}.

Table 2: Results for (a) exclusive $|V_{cb}|$ and (b) inclusive $|V_{cb}|$. The p115e223 is an abbreviation for Eq. (223) in page 115. The p5t2 is an abbreviation for Table 2 in page 5.

from analysis on $B_s \to D_s^* \ell \bar{\nu}$ decays which are not available in the B-factories. Since results for B_s decay channels have poor statistics, we drop out them here without loss of fairness. The rest of results for exclusive $|V_{cb}|$ have comparable size of errors and are consistent with one another within 1.0σ. In addition, we find that the results are consistent between the CLN and BGL analysis, after the clamorous debates [7, 22].

In Table 2 (b), we present recent results for inclusive $|V_{cb}|$. The Gambino group has reported updated results for inclusive $|V_{cb}|$ in 2021. There are a number of attempts to calculate inclusive $|V_{cb}|$ in lattice QCD, but they belong to a category of exploratory study rather than that of precision measurement yet [23].

PoS(CORFU2022)028

3.3 Input parameter ξ_0

The absorptive part of long distance effects on ε_K is parametrized into ξ_0.

$$\xi_0 = \frac{\text{Im}\, A_0}{\text{Re}\, A_0}, \qquad \xi_2 = \frac{\text{Im}\, A_2}{\text{Re}\, A_2}, \qquad \text{Re}\left(\frac{\varepsilon'}{\varepsilon}\right) = \frac{\omega}{\sqrt{2}|\varepsilon_K|}(\xi_2 - \xi_0)\,. \tag{17}$$

There are two independent methods to determine ξ_0 in lattice QCD: the indirect and direct methods. The indirect method is to determine ξ_0 using Eq. (17) with lattice QCD results for ξ_2 combined with experimental results for ε'/ε, ε_K, and ω. The direct method is to determine ξ_0 directly using the lattice QCD results for Im A_0, combined with experimental results for Re A_0.

In Table 3 (a), we summarize experimental results for Re A_0 and Re A_2. In Table 3 (b), we summarize lattice results for Im A_0 and Im A_2 calculated by RBC-UKQCD. In Table 3 (c), we summarize results for ξ_0 which is obtained using results in Table 3 (a) and (b).

Here, we use results of the indirect method for ξ_0 to evaluate ε_K, since its systematic and statistical errors are much smaller than those of the direct method.

parameter	method	value	Ref.	source
Re A_0	exp	$3.3201(18) \times 10^{-7}$ GeV	[30, 31]	NA
Re A_2	exp	$1.4787(31) \times 10^{-8}$ GeV	[30]	NA
ω	exp	$0.04454(12)$	[30]	NA
$\|\varepsilon_K\|$	exp	$2.228(11) \times 10^{-3}$	[32]	PDG-2021
Re $(\varepsilon'/\varepsilon)$	exp	$1.66(23) \times 10^{-3}$	[32]	PDG-2021

(a) Experimental results for ω, Re A_0 and Re A_2.

parameter	method	value (GeV)	Ref.	source
Im A_0	lattice	$-6.98(62)(144) \times 10^{-11}$	[33] p4t1	RBC-UK-2020
Im A_2	lattice	$-8.34(103) \times 10^{-13}$	[33] p31e90	RBC-UK-2020

(b) Results for Im A_0, and Im A_2 in lattice QCD.

parameter	method	value	ref	source
ξ_0	indirect	$-1.738(177) \times 10^{-4}$	[33]	SWME
ξ_0	direct	$-2.102(472) \times 10^{-4}$	[33]	SWME

(c) Results for ξ_0 obtained using the direct and indirect methods in lattice QCD.

Table 3: Results for ξ_0. Here, we use the same notation as in Table 2.

3.4 Input parameters: $\hat{B}_K$, ξ_{LD}, and others

In FLAG 2021 [18], they report lattice QCD results for $\hat{B}_K$ with $N_f = 2$, $N_f = 2+1$, and $N_f = 2+1+1$. Here, we use the results for $\hat{B}_K$ with $N_f = 2+1$, which is obtained by taking an average over the four data points from BMW 11, Laiho 11, RBC-UKQCD 14, and SWME 15 in Table 4 (a).

Collaboration	Ref.	$\hat{B}_K$
SWME 15	[34]	0.735(5)(36)
RBC/UKQCD 14	[35]	0.7499(24)(150)
Laiho 11	[36]	0.7628(38)(205)
BMW 11	[37]	0.7727(81)(84)
FLAG 2021	[18]	0.7625(97)

(a) $\hat{B}_K$

Input	Value	Ref.
G_F	$1.1663787(6) \times 10^{-5}$ GeV^{-2}	PDG-22 [38]
M_W	80.356(6) GeV	SM-22 [38]
θ	$43.52(5)^\circ$	PDG-22 [38]
m_{K^0}	497.611(13) MeV	PDG-22 [38]
ΔM_K	$3.484(6) \times 10^{-12}$ MeV	PDG-22 [38]
F_K	155.7(3) MeV	FLAG-21 [18]

(b) Other parameters

Table 4: (a) Results for $\hat{B}_K$ and (b) other input parameters.

The dispersive long distance (LD) effect is defined as

$$\xi_{\rm LD} = \frac{m'_{\rm LD}}{\sqrt{2}\Delta M_K}\,, \qquad m'_{\rm LD} = -\mathrm{Im}\left[\mathcal{P}\sum_C \frac{\langle \overline{K}^0|H_{\rm w}|C\rangle\langle C|H_{\rm w}|K^0\rangle}{m_{K^0}-E_C}\right] \tag{18}$$

As explained in Refs. [7], there are two independent methods to estimate $\xi_{\rm LD}$: one is the BGI estimate [39], and the other is the RBC-UKQCD estimate [40, 41]. The BGI method is to estimate the size of $\xi_{\rm LD}$ using chiral perturbation theory as follows,

$$\xi_{\rm LD} = -0.4(3) \times \frac{\xi_0}{\sqrt{2}} \tag{19}$$

The RBC-UKQCD method is to estimate the size of $\xi_{\rm LD}$ as follows,

$$\xi_{\rm LD} = (0 \pm 1.6)\%. \tag{20}$$

Here, we use both methods to estimate the size of $\xi_{\rm LD}$.

In Table 1 (b), we present higher order QCD corrections: η_{ij} with $i, j = t, c$. A new approach using $u - t$ unitarity instead of $c - t$ unitarity appeared in Ref. [42], which is supposed to have a better convergence with respect to the charm quark mass. But we have not incorporated this into our analysis yet, which we will do in near future.

In Table 4 (b), we present other input parameters needed to evaluate ε_K.

3.5 Input parameters: quark masses

In Table 5, we present the charm quark mass $m_c(m_c)$ and top quark mass $m_t(m_t)$. From FLAG 2021 [18], we take the results for $m_c(m_c)$ with $N_f = 2+1$, since there is some inconsistency among the lattice results of various groups with $N_f = 2 + 1 + 1$. For the top quark mass, we use the PDG 2022 results for the pole mass M_t to obtain $m_t(m_t)$.

In Table 6 (a), we plot top pole mass M_t as a function of time. Here we find that the average value drifts downward a little bit and the error shrinks fast as time goes on, thanks to accumulation of high statistics in the LHC experiments. The data for 2020 is dropped out intentionally to reflect on the absence of Lattice 2020 due to COVID-19.

Collaboration	N_f	$m_c(m_c)$	Ref.
FLAG 2021	$2+1$	1.275(5)	[18]
FLAG 2021	$2+1+1$	1.278(13)	[18]

(a) $m_c(m_c)$ [GeV]

Collaboration	M_t	$m_t(m_t)$	Ref.
PDG 2019	172.9(4)	163.08(38)(17)	[43]
PDG 2021	172.76(30)	162.96(28)(17)	[32]
PDG 2022	172.69(30)	162.90(28)(17)	[38]

(b) $m_t(m_t)$ [GeV]

Table 5: Results for (a) charm quark mass and (b) top quark mass.

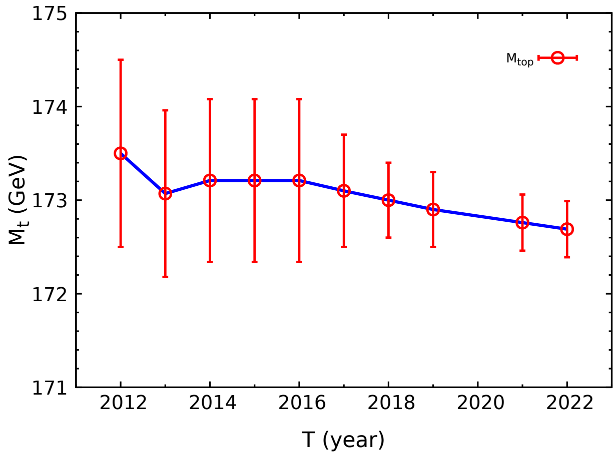

(a) History of M_t (top quark pole mass).

source	error (%)	memo
$\lvert V_{cb}\rvert$	49.7	Exclusive
η_{ct}	20.7	$c-t$ Box
$\bar{\eta}$	13.3	AOF
η_{cc}	8.7	$c-c$ Box
ξ_{LD}	2.1	RBC-UKQCD
$\bar{\rho}$	2.1	AOF
$\hat{B}_K$	1.7	FLAG
$\vdots$	$\vdots$	$\vdots$

(b) Error budget for $\lvert\varepsilon_K\rvert^{\text{SM}}$

Table 6: (a) M_t history (b) error budget.

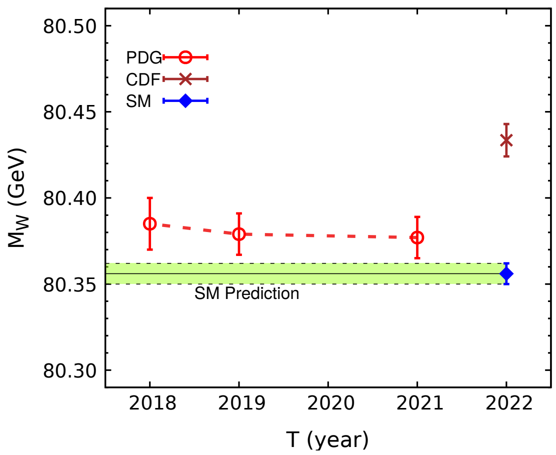

(a) History of M_W (W boson mass).

Source	M_W (GeV)	Ref.
SM-2022	80.356(6)	[38]
CDF-2022	80.4335(94)	[44]
PDG-2021	80.377(12)	[32]
PDG-2019	80.379(12)	[43]
PDG-2018	80.385(15)	[3]

(b) Table of M_W

Table 7: (a) M_W history (b) table of M_W.

3.6 Input parameters: W boson mass

In Fig. 7 (a), we plot M_W (W boson mass) as a function of time. The corresponding results for M_W are summarized in Table 7 (b). In Fig. 7 (a), the light-green band represents the standard model (SM) prediction, the red circles represents the PDG results, and the brown cross represents the CDF-2022 result. The upside is that the CDF-2022 result is the most precise and latest experimental

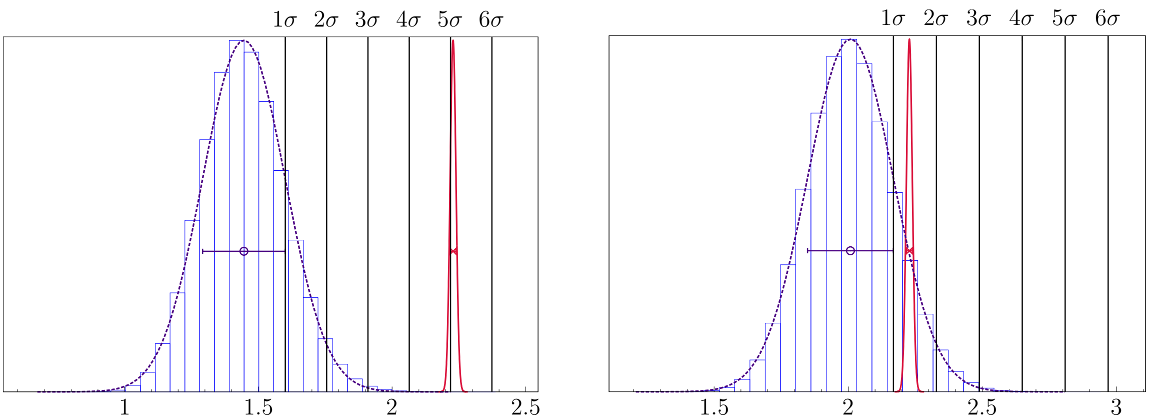

(a) Exclusive $|V_{cb}|$ (FNAL/MILC 2022, BGL) **(b)** Inclusive $|V_{cb}|$ (HFLAV 2021, 1S scheme)

Figure 1: $|\varepsilon_K|$ with (a) exclusive $|V_{cb}|$ (left) and (b) inclusive $|V_{cb}|$ (right) in units of 1.0×10^{-3}.

result for M_W. The downside, however, is that it has a 6.9σ tension from that of SM-2022 (the standard model prediction). Here, we use the SM-2022 result for M_W to evaluate ε_K.

4. Results for ε_K

In Fig. 1, we show results for $|\varepsilon_K|$ evaluated directly from the standard model (SM) with lattice QCD inputs given in the previous sections. In Fig. 1 (a), the blue curve represents the theoretical evaluation of $|\varepsilon_K|$ obtained using the FLAG-2021 results for $\hat{B}_K$, AOF for Wolfenstein parameters, the [FNAL/MILC 2022, BGL] results for exclusive $|V_{cb}|$, results for ξ_0 with the indirect method, and the RBC-UKQCD estimate for ξ_{LD}. The red curve in Fig. 1 represents the experimental results for $|\varepsilon_K|$. In Fig. 1 (b), the blue curve represents the same as in Fig. 1 (a) except for using the 1S scheme results for the inclusive $|V_{cb}|$.

Our results for $|\varepsilon_K|^{\text{SM}}$ and $\Delta\varepsilon_K$ are summarized in Table 8. Here, the superscript $^{\text{SM}}$ represents the theoretical expectation value of $|\varepsilon_K|$ obtained directly from the SM. The superscript $^{\text{Exp}}$ represents the experimental value of $|\varepsilon_K| = 2.228(11) \times 10^{-3}$. Results in Table 8 (a) are obtained using the RBC-UKQCD estimate for ξ_{LD}, and those in Table 8 (b) are obtained using the BGI estimate for ξ_{LD}. In Table 8 (a), we find that the theoretical expectation values of $|\varepsilon_K|^{\text{SM}}$ with lattice QCD inputs (with exclusive $|V_{cb}|$) has $5.12\sigma \sim 3.93\sigma$ tension with the experimental value of $|\varepsilon_K|^{\text{Exp}}$, while there is no tension with inclusive $|V_{cb}|$ (obtained using heavy quark expansion and QCD sum rules). We also find that the tension with inclusive $|V_{cb}|$ is small but keeps increasing with respect to time.

In Fig. 2 (a), we show the time evolution of $\Delta\varepsilon_K$ starting from 2012 till 2022. In 2012, $\Delta\varepsilon_K$ was 2.5σ, but now it is 5.05σ with exclusive $|V_{cb}|$ (FNAL/MILC-2022, BGL).[1] In Fig. 2 (b), we show the time evolution of the average $\Delta\varepsilon_K$ and the error $\sigma_{\Delta\varepsilon_K}$ during the period of 2012–2022.

At present, we find that the largest error ($\approx 50\%$) in $|\varepsilon_K|^{\text{SM}}$ comes from $|V_{cb}|$.[2] Hence, it is essential to reduce the errors in $|V_{cb}|$ as much as possible. To achieve this goal, there is an on-going

[1]Here, we use the results for exclusive $|V_{cb}|$ from FNAL/MILC-2022, since it contains the most comprehensive analysis on the $\bar{B} \to D^*\ell\bar{\nu}$ decays on both zero recoil and non-zero recoil data points, while it covers both BELL and BABAR experimental results.

[2]Refer to Table 6 (b) for more details.

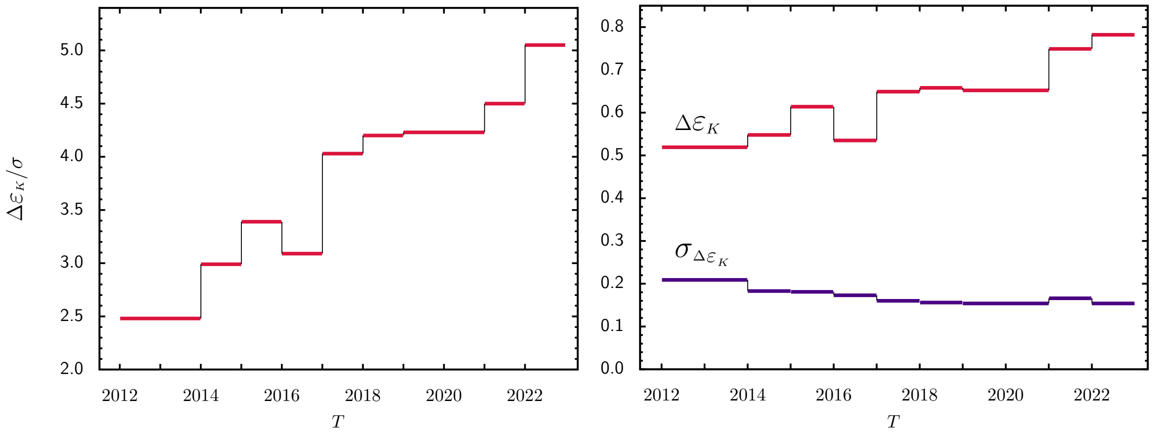

(a) Time evolution of $\Delta\varepsilon_K/\sigma$ **(b)** Time evolution of the average and error of $\Delta\varepsilon_K$

Figure 2: Time history of (a) $\Delta\varepsilon_K/\sigma$, and (b) $\Delta\varepsilon_K$ and $\sigma_{\Delta\varepsilon_K}$.

project to extract exclusive $|V_{cb}|$ using the Oktay-Kronfeld (OK) action for the heavy quarks to calculate the form factors for $\bar{B} \to D^{(*)}\ell\bar{\nu}$ decays [45–51].

A large portion of interesting results for $|\varepsilon_K|^{\rm SM}$ and $\Delta\varepsilon_K$ could not be presented in Table 8 and in Fig. 2 due to lack of space: for example, results for $|\varepsilon_K|^{\rm SM}$ obtained using exclusive $|V_{cb}|$ (FLAG 2021), results for $|\varepsilon_K|^{\rm SM}$ obtained using ξ_0 determined by the direct method, and so on. We plan to report them collectively in Ref. [52].

$\lvert V_{cb}\rvert$	method	reference	$\lvert\varepsilon_K\rvert^{\rm SM}$	$\Delta\varepsilon_K$
exclusive	BGL	BELLE 2021	1.518 ± 0.180	3.93σ
exclusive	CLN	BELLE 2021	1.532 ± 0.171	4.07σ
exclusive	BGL	BABAR 2019	1.441 ± 0.166	4.72σ
exclusive	CLN	BABAR 2019	1.446 ± 0.161	4.86σ
exclusive	BGL	FNAL/MILC 2022	1.446 ± 0.154	5.05σ
exclusive	CLN	HFLAV 2021	1.566 ± 0.142	4.63σ
inclusive	kinetic	Gambino 2021	2.041 ± 0.168	1.12σ
inclusive	1S	HFLAV 2021	2.008 ± 0.160	1.37σ

(a) RBC-UKQCD estimate for $\xi_{\rm LD}$

$\lvert V_{cb}\rvert$	method	reference	$\lvert\varepsilon_K\rvert^{\rm SM}$	$\Delta\varepsilon_K$
exclusive	BGL	FNAL/MILC 2022	1.494 ± 0.157	4.66σ
exclusive	CLN	HFLAV 2021	1.614 ± 0.145	4.22σ

(b) BGI estimate for $\xi_{\rm LD}$

Table 8: $|\varepsilon_K|$ in units of 1.0×10^{-3}, and $\Delta\varepsilon_K = |\varepsilon_K|^{\rm Exp} - |\varepsilon_K|^{\rm SM}$.

Acknowledgments

We thank Jon Bailey, Yong-Chull Jang, Stephen Sharpe, and Rajan Gupta for helpful discussion. We thank Guido Martinelli for providing us the most updated results of the UTfit Collaboration in time. The research of W. Lee is supported by the Mid-Career Research Program (Grant No. NRF-2019R1A2C2085685) of the NRF grant funded by the Korean government (MSIT). W. Lee would like to acknowledge the support from the KISTI supercomputing center through the strategic support program for the supercomputing application research (No. KSC-2018-CHA-0043, KSC-2020-CHA-0001, KSC-2023-CHA-0010). Computations were carried out in part on the DAVID cluster at Seoul National University.

References

[1] G. Buchalla, A.J. Buras and M.E. Lautenbacher*Rev. Mod. Phys.* **68** (1996) 1125 [hep-ph/9512380].

[2] A.J. Buras hep-ph/9806471.

[3] C. Patrignani et al.*Chin. Phys.* **C40** (2016) 100001.

[4] SWME collaboration, *2022 Update on ε_K with lattice QCD inputs*, *PoS* **LATTICE2022** (2022) 297 [2301.12375].

[5] SWME collaboration, *2021 update on ε_K with lattice QCD inputs*, *PoS* **LATTICE2021** (2021) 078 [2202.11473].

[6] LANL-SWME collaboration*PoS* **LATTICE2019** (2019) 029 [1912.03024].

[7] J.A. Bailey et al.*Phys. Rev.* **D98** (2018) 094505 [1808.09657].

[8] J.A. Bailey, Y.-C. Jang, W. Lee and S. Park*Phys. Rev.* **D92** (2015) 034510 [1503.05388].

[9] J.A. Bailey et al.*PoS* **LATTICE2018** (2018) 284 [1810.09761].

[10] Y.-C. Jang, W. Lee, S. Lee and J. Leem*EPJ Web Conf.* **175** (2018) 14015 [1710.06614].

[11] J.A. Bailey, Y.-C. Jang, W. Lee and S. Park*PoS* **LATTICE2015** (2015) 348 [1511.00969].

[12] T. Inami and C. Lim*Prog.Theor.Phys.* **65** (1981) 297.

[13] S. Herrlich and U. Nierste*Nucl.Phys.* **B476** (1996) 27 [hep-ph/9604330].

[14] J. Charles et al.*Eur.Phys.J.* **C41** (2005) 1 [hep-ph/0406184].

[15] M. Bona et al.*JHEP* **10** (2006) 081 [hep-ph/0606167].

[16] B. Winstein and L. Wolfenstein*Rev.Mod.Phys.* **65** (1993) 1113.

[17] A. Bevan, M. Bona, M. Ciuchini, D. Derkach, E. Franco et al.*Nucl.Phys.Proc.Suppl.* **241-242** (2013) 89.

PoS(CORFU2022)028

[18] Flavour Lattice Averaging Group (FLAG) collaboration*Eur. Phys. J. C* **82** (2022) 869 [2111.09849].

[19] UTfit collaboration 2212.03894.

[20] A.J. Buras and D. Guadagnoli*Phys.Rev.* **D78** (2008) 033005 [0805.3887].

[21] J. Brod and M. Gorbahn*Phys.Rev.* **D82** (2010) 094026 [1007.0684].

[22] Fermilab Lattice, MILC collaboration*Eur. Phys. J. C* **82** (2022) 1141 [2105.14019].

[23] A. Barone, A. Jüttner, S. Hashimoto, T. Kaneko and R. Kellermann, *Inclusive semi-leptonic $B_{(s)}$ mesons decay at the physical b quark mass*, *PoS* **LATTICE2022** (2023) 403 [2211.15623].

[24] HFLAV collaboration*Eur. Phys. J. C* **81** (2021) 226 [1909.12524].

[25] Belle collaboration*Phys. Rev. D* **100** (2019) 052007 [1809.03290].

[26] BaBar collaboration*Phys. Rev. Lett.* **123** (2019) 091801 [1903.10002].

[27] LHCb collaboration*Phys. Rev. D* **101** (2020) 072004 [2001.03225].

[28] M. Bordone, B. Capdevila and P. Gambino*Phys. Lett. B* **822** (2021) 136679 [2107.00604].

[29] P. Gambino, K.J. Healey and S. Turczyk*Phys. Lett.* **B763** (2016) 60 [1606.06174].

[30] T. Blum et al.*Phys. Rev.* **D91** (2015) 074502 [1502.00263].

[31] Z. Bai et al.*Phys. Rev. Lett.* **115** (2015) 212001 [1505.07863].

[32] Particle Data Group collaboration*PTEP* **2020** (2020) 083C01.

[33] RBC, UKQCD collaboration*Phys. Rev. D* **102** (2020) 054509 [2004.09440].

[34] B.J. Choi et al.*Phys. Rev.* **D93** (2016) 014511 [1509.00592].

[35] T. Blum et al.*Phys. Rev.* **D93** (2016) 074505 [1411.7017].

[36] J. Laiho and R.S. Van de Water*PoS* **LATTICE2011** (2011) 293 [1112.4861].

[37] S. Durr et al.*Phys. Lett.* **B705** (2011) 477 [1106.3230].

[38] Particle Data Group collaboration*PTEP* **2022** (2022) 083C01.

[39] A.J. Buras, D. Guadagnoli and G. Isidori*Phys.Lett.* **B688** (2010) 309 [1002.3612].

[40] N. Christ et al.*Phys.Rev.* **D88** (2013) 014508 [1212.5931].

[41] N. Christ et al.*PoS* **LATTICE2013** (2014) 397 [1402.2577].

[42] J. Brod, M. Gorbahn and E. Stamou*Phys. Rev. Lett.* **125** (2020) 171803 [1911.06822].

[43] M. Tanabashi et al.*Phys. Rev.* **D98** (2018) 030001.

[44] CDF collaboration*Science* **376** (2022) 170.

[45] T. Bhattacharya, B.J. Choi, R. Gupta, Y.-C. Jang, S. Jwa, S. Lee et al.*PoS* **LATTICE2021** (2021) 136 [2204.05848].

[46] LANL-SWME collaboration*PoS* **LATTICE2019** (2020) 050 [2002.04755].

[47] LANL/SWME collaboration*PoS* **LATTICE2019** (2020) 056 [2003.09206].

[48] T. Bhattacharya et al.*PoS* **LATTICE2018** (2018) 283 [1812.07675].

[49] J.A. Bailey et al.*EPJ Web Conf.* **175** (2018) 13012 [1711.01786].

[50] J. Bailey, Y.-C. Jang, W. Lee and J. Leem*EPJ Web Conf.* **175** (2018) 14010 [1711.01777].

[51] LANL-SWME collaboration*Phys. Rev. D* **105** (2022) 034509 [2001.05590].

[52] SWME collaboration, J. Bailey, J. Kim, S. Lee, W. Lee, Y.-C. Jang, J. Leem et al.